2008 IEEE International Conference on
Robotics and Automation
Pasadena, CA, USA, May 19-23, 2008

Hybrid Simulation of a Dual-Arm Space Robot Colliding with a Floating Object

Ryohei Takahashi, Hiroto Ise,
Atsushi Konno and Masaru Uchiyama
Department of Aerospace Engineering,
Tohoku University
Aoba-yama 6-6-01, Sendai 980-8579, Japan
{*ryohei, konno, uchiyama*}*@space.mech.tohoku.ac.jp*

Daisuke Sato
Department of Mechanical Systems
Engineering, Musashi Institute of Technology
Tamazutsumi 1-28-1, Setagaya,
Tokyo 158-8557, Japan
dsato@sc.musashi-tech.ac.jp

***Abstract*— In order to verify orbital operations of a dual-arm space robot on the ground, a hybrid simulator (hardware in the loop simulator) is developed. The hybrid simulator includes a 14-degrees-of-freedom (14-DOF) dual-arm robot and 9-DOF motion table. A hybrid simulator has a great advantage in simulating complicated collision with multiple contacts, because it is difficult for a numerical simulation to get reliable and accurate results of such complicated phenomena. In this paper, the system architecture and the motion planning for three motion tables are presented. Two experiments are performed to confirm the basic motion and simulate a free-flying dual-arm space robot colliding with a floating object. The feasibility of robot operation is discussed from showing the position and force data obtained in the motion simulation.**

***Index Terms*— Hybrid simulation, Dual-arm space robot.**

I. Introduction

Recently, space technology is actively developed, and it is expected for space robots to carry out services on orbit such as construction or maintenance of space systems. Single-arm space robots have been used so far in orbital operations, but the operation is limited to relatively simple tasks. Therefore, it is expected for a dual-arm space robot to perform more complicated tasks. In order to develop these space robot technologies, the feasibility and reliability of robot system to perform orbital operations have to be verified by repetitive operation tests. However, it is almost impossible to verify them on orbit, because unreliable and untested operations are forbidden in space for safety. So it is expected to emulate a micro-gravity environment, and test space robot's operation on the earth. As a method to emulate a micro-gravity environment, hybrid simulation (hardware in the loop simulation) has a lot of advantages. Therefore, a considerable number of researches have been made on hybrid simulation [1]–[5].

Inoue et al. developed a docking simulator to simulate docking motion of spacecrafts [6]. Shimoji et al. developed Berthing Dynamics Simulator (BDS), and simulated capturing operation of a floating object by a single-arm space robot [7]. Ejiri et al. developed Advanced Space Robot Testbed with Redundant Arms (ASTRA), and simulated capturing operation of a spinning satellite by a dual-arm space robot [8]. The motion table of the ASTRA system has two translational and one rotational degrees-of-freedom (DOF) for both of the target object and the two-armed space robot. Therefore, the relative motion between the spinning satellite and the two-armed space robot in the ASTRA system is limited to planar motion. Nishimaki developed a hybrid simulator which is composed of a serial 7-DOF robot arm and a 6-DOF parallel motion table [9]. The hybrid simulator presented in [9] has only a single arm, and hence, it is impossible to simulate two arms operation.

This research was supported by the Ministry of Education, Science, Sports and Culture, Grant-in-Aid for Scientific Research (A), 16206024.

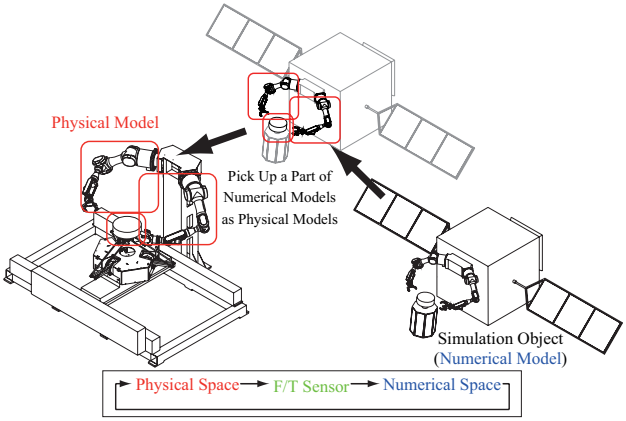

Fig. 1. Concept of the hybrid simulation.

In order to simulate two arms operation on orbit, a hybrid simulator which is composed of a dual-arm robot and a 9-DOF motion table is developed. The motion table consists of a 2-DOF X-Y motion table, a 6-DOF HEXA [10] motion table and 1-DOF spin motion table. This paper presents the system architecture of the developed hybrid simulator. Using the hybrid simulator, a motion of a dual-arm space robot colliding with a floating object is simulated. Showing the result of the hybrid simulation, the validity of the simulator is discussed in this paper.

II. Hybrid Simulator

A. Hybrid Simulation

Hybrid simulation is a method that combines a hardware experiment with a numerical simulation. The hardware experiment utilizes the same hardware model used in actual orbital operation under the artificially created micro-gravity environment. The numerical simulation utilizes a spacecraft

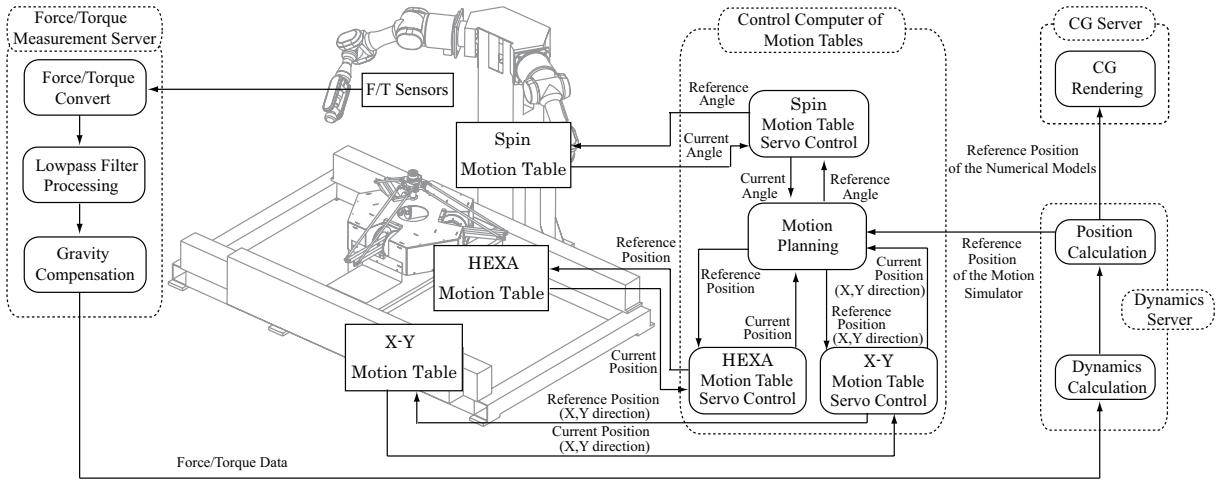

Fig. 2. A system block diagram for the hybrid simulator.

model and micro-gravity environment built in the computer. Hybrid simulation is basically numerical simulation, replacing a part of numerical model by the corresponding hardware (physical model), in order to test complicated motion such as interaction and collision. Force/torque sensors are attached on the border between a physical model and a numerical model. External forces and moments that affect on the physical model are measured by the force/torque sensors. Considering the measured external forces and moments as inputs to the numerical model, the forward dynamics is solved. The relative motion between the space robot and the target object calculated from the forward dynamics is demonstrated by the motion table in real time.

Thus, in hybrid simulation, motion involving interaction and collision is experimented using actual hardware, and resultant motion is numerically simulated. The concept of hybrid simulation is illustrated in Fig. 1. The flow of the hybrid simulation is summarized as follows:

Step 1: Relative position and orientation between the numerical models are derived from initial conditions. After that, position and orientation of the physical model of the target object are calculated.

Step 2: Motion of the physical model of the target object is demonstrated by the motion table.

Step 3: Force and moment generated by contact between the physical hand and object are measured by the force/torque sensors.

Step 4: Forward dynamics is calculated using the numerical models and the measured force and moment data. The forward dynamics produces relative position and orientation between the numerical models.

Step 5: Position and orientation of the physical model are demonstrated by the motion table based upon the motion of the numerical models generated by solving the forward dynamics.

Step 6: Motion of the numerical models is visualized by computer graphics (CG).

Step 7: Go back to Step 3 if simulation continues.

In the hybrid simulation, force and moment are generated by a hardware experiment using the physical models and are measured by the attached force/torque sensors. In general, a numerical simulation is the easiest way to simulate a space robot operation. However, there is no guarantee that result of the numerical simulation is reliable and accurate enough, because there is a difficulty in simulating complicated phenomena such as simultaneous multiple contacts. Therefore, a hardware experiment is desired to get a reliable result. However, a full hardware simulation is not realistic, because large and massive equipment such as a water tank is needed to cancel the gravity. Consequently, the hybrid simulation is a realistic solution.

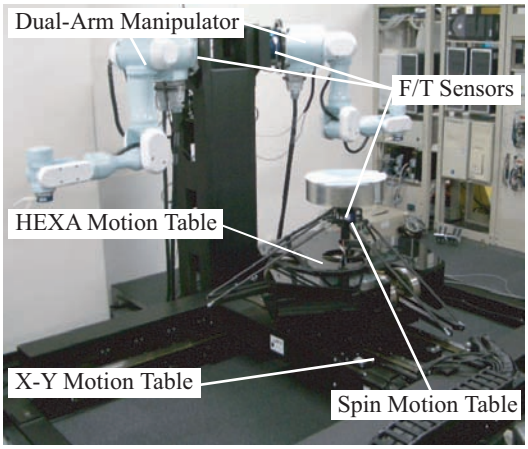

Fig. 3. Overview of the hybrid simulator.

B. System Configuration

System configuration and overview of the simulator are shown in Figs. 2 and 3, respectively. As described in Introduction, the motion table consists of an X-Y motion table, a HEXA motion table and a spin motion table. The spin motion table is mounted on the HEXA motion table, and demonstrates a spinning object. The HEXA [10] motion table is mounted on the X-Y motion table, and demonstrates six dimensional relative motion between the dual-arm space robot and the target object. The X-Y motion table carries the HEXA motion table, and demonstrates slow and wide-ranging motion in X-Y plane. A 6-axis force/torque sensor

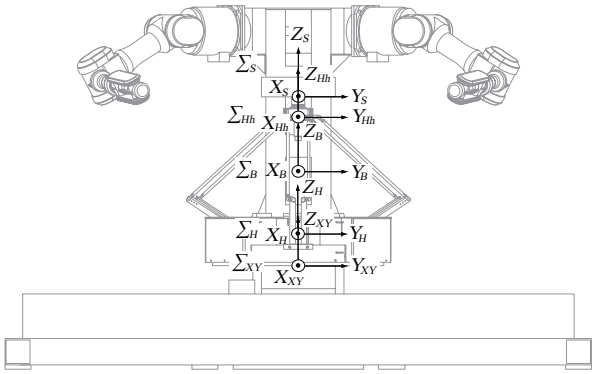

Fig. 4. Coordinate systems of the hybrid simulator.

is attached to the end-effector of the HEXA motion table. A physical model which is a part of a target object is mounted on the spin motion table. Thus, force and moment acting on the physical model is measured by the force/torque sensor. Furthermore, two 6-axis force/torque sensors are mounted on the proximal end of each arm. Therefore, reaction force caused by moving arms and external force exerted by contact between arms and object are measured by the two force/torque sensors.

In the hybrid simulator system, four computers are used. They are used for measuring force and moment, solving the forward dynamics using the numerical models, controlling motion tables and drawing CG. The hybrid simulation requires a high computational power, however, processes in the hybrid simulation are distributed to the four computers, and hence, one cycle of the simulation finishes within 1 ms. The sampling period is set to 1 ms.

III. Motion Demonstration

A. Motion Planning

Coordinate systems of the hybrid simulator are shown in Fig. 4. Σ_B is the absolute coordinate system, Σ_{XY} is the coordinate system fixed on the X-Y motion table, Σ_H and Σ_{Hh} are the coordinate systems fixed on the base and the end-effector of the HEXA motion table, respectively. Σ_S is the coordinate system fixed on the spin motion table.

The 9-DOF motion table has redundancy; 1-DOF around Z_{Hh} axis and 2-DOF in X_H-Y_H plane. Therefore, the redundancy must be solved in the motion planning for the 9-DOF motion table. The main advantage of the HEXA motion table is the quickness in motion. In order to make the most use of the advantage, the following strategy is applied to the motion planning.

The relative motion between the numerical models obtained by solving the forward dynamics is divided in the frequency domain. In order to divide the motion in the frequency domain, the Chebyshev II type lowpass filter is used, whose cut off frequency is 1.0 Hz. The filtered motion (low frequency motion) in the X_B-Y_B plane is assigned to the X-Y motion table, while the low frequency motion around the Z_B axis is assigned to the spin motion table. The remained motion is assigned to the HEXA motion table. As a result of this assignment, the HEXA motion table mainly demonstrates instantaneous high frequency phenomenon after a collision, while the other motion tables mainly demonstrates low frequency wide range motion.

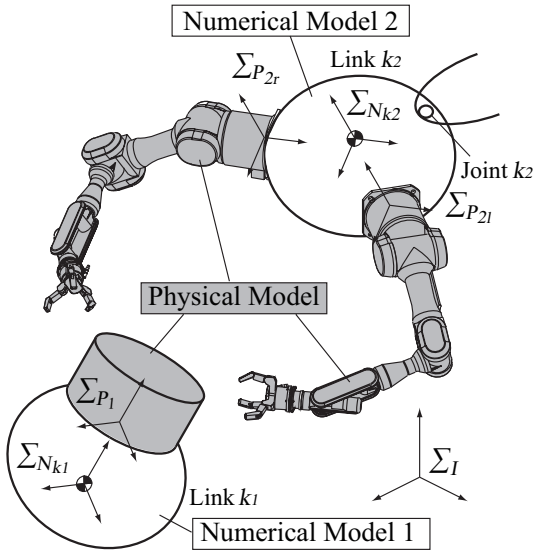

Fig. 5. Coordinate systems of the physical and the numerical models. White objects are the numerical models. Gray objects are the physical models.

B. Demonstration of Relative Motion

The purpose of the hybrid simulation is to test orbital operations performed by a dual-arm space robot. Each arm has force/torque sensors at the wrist and shoulder. A mechanical part that has a force/torque sensor at its proximal end can be a physical model, and thus, the hand can be a physical model. However, two arms are considered as physical models in this work as illustrated in Fig. 5. Since the bases of the space robot and the target object are numerical models, any conditions can be simulated such as the robot is floating, the robot is mounted on a flexible structure, the robot is mounted on a rigid base, and so on. Hereinafter, the detailed method of the hybrid simulation is described.

Coordinate systems of physical models and numerical models are shown in Fig. 5. The models of the target object and the base of the space robot are named numerical model 1 and numerical model 2, respectively. Σ_I is an absolute coordinate system for numerical models, $\Sigma_{N_{k_1}}$ and $\Sigma_{N_{k_2}}$ are coordinate systems fixed on the link k_1 and link k_2, respectively. The link k_1 and link k_2 are links that are connected to the physical models. Σ_{P_1} is a coordinate system fixed on the physical model of a target object, and $\Sigma_{P_{2_r}}$ and $\Sigma_{P_{2_l}}$ are coordinate systems fixed on the right arm and left arm, respectively.

After a collision between the dual-arm and target object, force and moment acting on physical models are measured by the force/torque sensors. Force and moment acting on the center of mass (CoM) of link k_1 are expressed by equation (1):

$$\begin{bmatrix} {}^{N_{k_1}}\boldsymbol{f} \\ {}^{N_{k_1}}\boldsymbol{n} \end{bmatrix} = \begin{bmatrix} {}^{P_1}_{N_{k_1}}\boldsymbol{R}^T & \boldsymbol{0} \\ {}^{N_{k_1}}_{P_1}\tilde{\boldsymbol{p}}\,{}^{P_1}_{N_{k_1}}\boldsymbol{R}^T & {}^{P_1}_{N_{k_1}}\boldsymbol{R}^T \end{bmatrix} \begin{bmatrix} {}^{P_1}\boldsymbol{f} \\ {}^{P_1}\boldsymbol{n} \end{bmatrix}, \quad (1)$$

$$ {}^{N_{k_1}}_{P_1}\tilde{\boldsymbol{p}} = \begin{bmatrix} 0 & -p_z & p_y \\ p_z & 0 & -p_x \\ -p_y & p_x & 0 \end{bmatrix}, \tag{2} $$

where ${}^{N_{k_1}}\boldsymbol{f}$ and ${}^{N_{k_1}}\boldsymbol{n}$ are force and moment acting on the CoM of link k_1, respectively, ${}^{P_1}\boldsymbol{f}$ and ${}^{P_1}\boldsymbol{n}$ are force and moment expressed in Σ_{P_1}, which are transferred from force and moment measured by the force/torque sensor on the end-effector of the HEXA motion table, respectively, ${}^{P_1}_{N_{k_1}}\boldsymbol{R}$ is a rotational matrix from $\Sigma_{N_{k_1}}$ to Σ_{P_1}, and ${}^{N_{k_1}}_{P_1}\boldsymbol{p}$ is position vector from the origin of $\Sigma_{N_{k_1}}$ to origin of Σ_{P_1}. Also, ${}^{N_{k_1}}_{P_1}\tilde{\boldsymbol{p}}$ expressed in equation (2) is a skew-symmetric matrix and ${}^{N_{k_1}}_{P_1}\boldsymbol{p} = [p_x \;\; p_y \;\; p_z]^T$ is defined.

After a collision between the dual-arm and target object, force and moment acting on the left and right arms are measured by two force/torque sensors attached between each arm and a base. In the same way for numerical model 1, using equation (1) and (2), force and moment measured by each sensor are transferred with respect to $\Sigma_{N_{k_2}}$. The force and moment acting on the CoM of link k_2 are expressed by:

$$ \begin{bmatrix} {}^{N_{k_2}}\boldsymbol{f} \\ {}^{N_{k_2}}\boldsymbol{n} \end{bmatrix} = \begin{bmatrix} {}^{N_{k_2}}\boldsymbol{f}_l + {}^{N_{k_2}}\boldsymbol{f}_r \\ {}^{N_{k_2}}\boldsymbol{n}_l + {}^{N_{k_2}}\boldsymbol{n}_r \end{bmatrix}, \tag{3} $$

where ${}^{N_{k_2}}\boldsymbol{f}$ and ${}^{N_{k_2}}\boldsymbol{n}$ are force and moment acting on the CoM of link k_2, respectively. ${}^{N_{k_2}}\boldsymbol{f}_l$, ${}^{N_{k_2}}\boldsymbol{n}_l$, ${}^{N_{k_2}}\boldsymbol{f}_r$ and ${}^{N_{k_2}}\boldsymbol{n}_r$ are forces and moments acting on the CoM of link k_2 through the left and right arm, respectively. Considering the calculated ${}^{N_{k_1}}\boldsymbol{f}$, ${}^{N_{k_1}}\boldsymbol{n}$, ${}^{N_{k_2}}\boldsymbol{f}$ and ${}^{N_{k_2}}\boldsymbol{n}$ as external forces and moments, the forward dynamics is computed using the order n Rosenthal algorithm [11]. Then, ${}^{N_{k_1}}\boldsymbol{p}$ which is position vector from the origin of $\Sigma_{N_{k_1}}$ to origin of Σ_I and ${}^{N_{k_1}}\boldsymbol{R}$ which is a rotational matrix from Σ_I to $\Sigma_{N_{k_1}}$ are calculated by executing Euler's numerical integration and forward kinematics calculation of each link. ${}^{N_{k_2}}\boldsymbol{p}$ and ${}^{N_{k_2}}\boldsymbol{R}$ are calculated in the same way. As a result, relative position and orientation between links k_1 and k_2 are expressed as follows:

$$ \boldsymbol{p}_R = {}^{N_{k_2}}\boldsymbol{p} - \boldsymbol{R}_R \, {}^{N_{k_1}}\boldsymbol{p} \,, \tag{4} $$

$$ \boldsymbol{R}_R = {}^{N_{k_2}}\boldsymbol{R} \, {}^{N_{k_1}}\boldsymbol{R}^T \,, \tag{5} $$

where $\boldsymbol{p}_R$ is vector which expresses relative position between links k_1 and k_2, and $\boldsymbol{R}_R$ is a rotational matrix which expresses relative orientation between links k_1 and k_2. $\boldsymbol{p}_R$ and $\boldsymbol{R}_R$ are expressed with respect to $\Sigma_{N_{k_2}}$. Reference motion for the motion table is calculated to realize relative position and orientation between numerical models expressed by equations (4) and (5). The reference motion is divided in the frequency domain, and assigned for each motion table as described in Section IIIA.

IV. Preliminary Experiment on Hybrid Simulation

A. Scenario for the Experiment

In order to verify the hybrid simulation described in Sections II and III, preliminary experiment on hybrid simulation is performed.

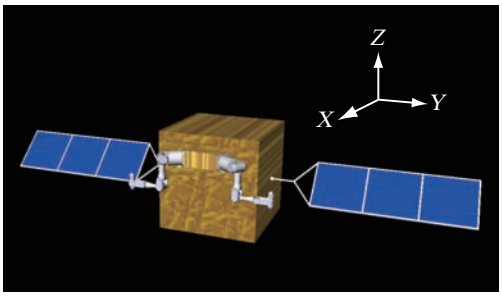

Fig. 6. Numerical model of the satellite equipped with two robot arms.

TABLE I
Mass and inertia parameters of the satellite.

Mass [kg]	Inertia [kg·m^2]
1000.0	diag[908.558 420.098 925.730]

In the experiment, a free-flying dual-arm space robot is assumed. An external force generated by pushing the left shoulder of a dual-arm by a human hand is acting on the dual-arm space robot. After pushing the left shoulder, the space robot moves in the force and moment directions. So in the experiment, demonstration of relative motion by the motion table between the dual-arm space robot and the target object is verified. No control command is given to the dual-arm, and therefore, it keeps the initial position and orientation. In addition, though the uniaxial rotating object is used as the target object, force and moment are not acted on. Thus, motion of the dual-arm space robot is only regarded.

The satellite is used as a numerical model, shown in Fig. 6. Body of the satellite is cube 1.6 m on a side. This satellite is equipped with two 7-DOF manipulators and two solar arrays. Mass and inertia parameters of the satellite are shown in TABLE I.

B. Experimental Results

Experimental results are shown in Figs. 7 and 8. Figs. 7 (a) and (b) show force acting on the CoM of the satellite in the Y direction and moment around the X axis, respectively. Figs. 8 (a) and (b) show relative position between the satellite and the target object in the Y direction and relative roll angle, respectively. The relative position and orientation are expressed with respect to $\Sigma_{N_{k_2}}$ which is fixed on the CoM of the satellite, and X-Y-Z Euler angle is applied to express orientation.

Shown in Figs. 7 and 8, the direction of transition of relative position and orientation is opposite direction of force and moment applied on the CoM of the satellite, respectively. After an external force and moment were applied on the left shoulder, the satellite moved translationally in the direction of the applied force, and moved rotationally in the direction of the applied moment. Furthermore, in the experiment, the target object remains stationary. Thus, the direction of motion of the target object observed from the satellite is opposite direction of motion of the satellite. Therefore, the experimental result indicates this appearance, and demonstration of relative motion between a free-flying dual-arm space robot and a target object is verified.

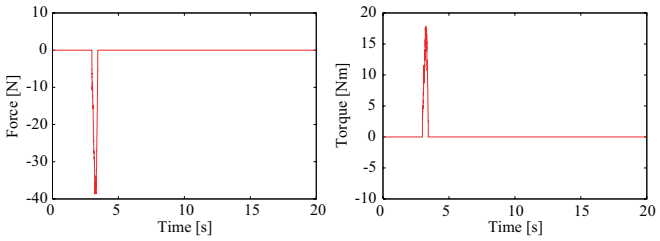

(a) (b)

Fig. 7. Input force and moment to the numerical model: (a) in the Y direction, (b) in the roll direction.

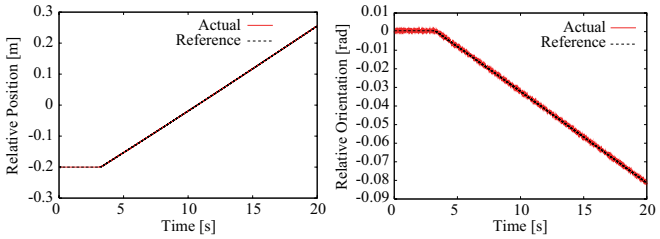

(a) (b)

Fig. 8. Relative position and orientation between the numerical models: (a) in the Y direction, (b) in the roll direction.

V. Hybrid Simulation of Hand-Object Collision

A. Scenario for the Hybrid Simulation

The hybrid simulation of a free-flying dual-arm space robot colliding with a floating object is performed.

The same satellite used in preliminary experiment on hybrid simulation is also used as a free-flying dual-arm space robot. A CG image and parameters of the satellite are shown in Fig. 6 and TABLE I, respectively. The circular cylinder shown in Fig. 9 (a) is a numerical model of a floating object. The radius and height of the floating object are 0.17 m and 0.135 m, respectively. The physical model which is a part of the floating object is mounted on the end-effector of the spin motion table. The overview of the physical model of the floating object is shown in Fig. 9 (b). A spherical end-effector is attached to the distal end of the left arm to make a point contact with the physical model of the floating object. Mass and inertia parameters of the floating object are shown in TABLE II.

In the experiment, the left arm of the satellite is moved and the end-effector of the left arm collides with the physical model of the floating object. The initial states of the satellite and floating object are stationary. Accuracy of the hybrid simulation is evaluated by the experimental result.

B. Experimental Results

Sequential photographs of the hybrid simulation are shown in Fig. 10. After about 10 s from the start of the hybrid simulation, the spherical end-effector of the left arm collides with the physical model of the floating object. Then relative motion between the satellite and the floating object caused by the collision is demonstrated by the motion table.

Results of the experiment are plotted in Fig. 11. Figs. 11 (a), (b), (c) and (d) show relative position between the satellite and the floating object in the X and Y directions,

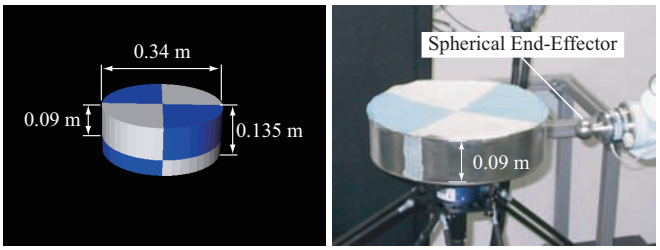

(a) (b)

Fig. 9. The numerical and the physical models of the floating object: (a) the numerical model, (b) the physical model.

TABLE II

Mass and Inertia Parameters of the Floating Object.

Mass [kg]	Inertia [kg·m^2]
350.0	diag[20.310 20.310 32.891]

and relative roll and pitch angles, respectively. The relative position and orientation are expressed with respect to $\Sigma_{N_{k_2}}$ which is fixed on the CoM of the satellite. Before the collision between the left hand and the floating object, the satellite remains stationary though left arm is moved. After the collision, both the satellite and the floating object move and relative motion between them is demonstrated by the motion table. A random spike shown in the actual data of Figs. 11 (c) and (d) is caused by a disturbance of the collision. It is needed to eliminate this spike by improving a control law of the motion table. However, position error of the end-effector of motion table is less than 1 mm, and orientation error is less than 0.01 rad in each direction including the Z and yaw directions. Thus, it is confirmed that the motion table accurately follows desired trajectory and this simulator is effective to simulate motion under micro-gravity environment.

Next, accuracy of this simulator is discussed. In the experiment, the CoM of the sphere of the end-effector and the floating object is corresponded in the X and Z direction. Moreover, the spherical end-effector of the left arm moves along the Y axis. Therefore, it is expected that the floating object moves strictly in the negative direction of the Y axis after the collision. However in the experiment, the floating object moves not only in the Y direction but also in the X, roll, pitch and yaw direction after the collision. In fact, displacements in the X, roll, pitch and yaw direction were 0.1 mm, 0.01 rad, 0.02 rad and 0.025 rad, respectively.

This is caused by error due to parts misalignment and servo error of the dual-arm and motion table. At the moment of the collision, the CoM of the sphere of the end-effector and the floating object does not correspond perfectly in the X and Z direction. As a result, translational motion in the X direction and rotational motion was generated by the misalignment. Therefore, it is expected to calibrate to remove the misalignment in order for an accurate simulation. In addition, consistency between actual motion under micro-gravity environment and motion demonstrated by the hybrid simulator is needed to evaluate.

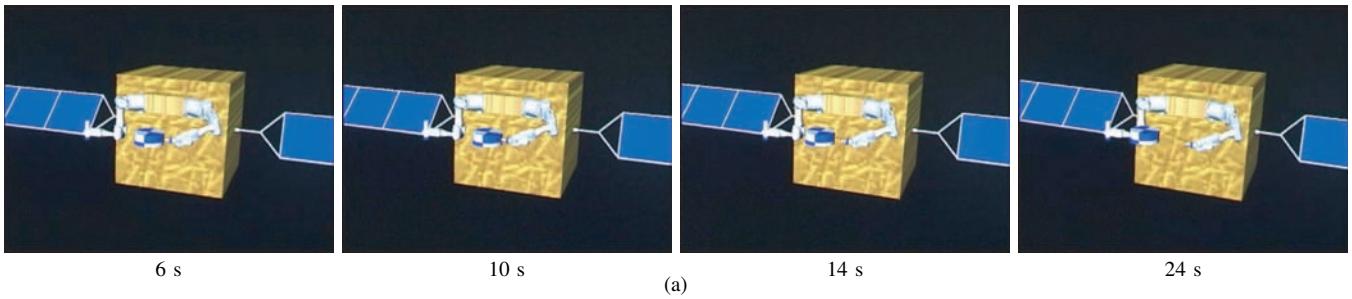

Fig. 10. Motion simulation of a dual-arm space robot colliding with a floating object: (a) CG, (b) motion table. (6 s: before the collision, 10 s: the moment of the collision, 14 s: after the collision, 24 s: end of simulation.)

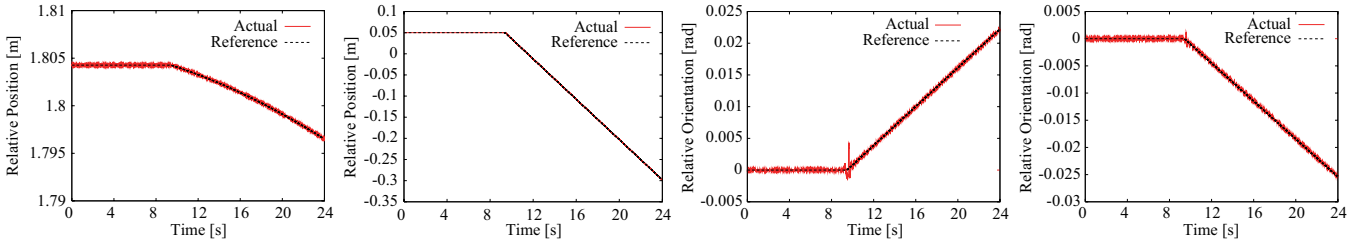

Fig. 11. Relative position and orientation of the numerical models: (a) in the X direction, (b) in the Y direction, (c) in the roll direction, (d) in the pitch direction.

VI. Conclusions

In this paper, the system architecture of the hybrid simulator which demonstrates 6-DOF relative motion between a dual-arm space robot and a target object is described. Motion generation method of the motion table is discussed and basic performance of the hybrid simulator is confirmed by preliminary experiment of motion demonstration. Moreover, assuming actual orbital operation, the experiment of a free-flying dual-arm space robot colliding with a floating object is performed. From this experimental result, validity of this hybrid simulator in simulating motion under micro-gravity environment is confirmed.

The main goal of this hybrid simulator is to simulate orbital operations by a dual-arm space robot. As a future work, actual orbital operations such as a capturing a damaged satellite task are planned to perform.

References

[1] K. Yoshida, H. Nakanishi, H. Ueno, N. Inaba, T. Nishimaki and M. Oda, "Dynamics, control and impedance matching for robotic capture of a non-cooperative satellite," *Advanced Robotics*, Vol. 18, No. 2, pp. 175–198, 2004.

[2] G. Rouleau, I. Rekleitis, R. L'Archevêque, E. Martin, K. Parsa and E. Dupuis, "Autonomous Capture of a Tumbling Satellite," in *Proc. of 2006 IEEE Int. Conf. on Robotics and Automation*, pp. 3855–3860, 2006.

[3] F. Aghili, M. Namvar and G. Vukovich, "Satellite Simulator with a Hydraulic Manipulator," in *Proc. of 2006 IEEE Int. Conf. on Robotics and Automation*, pp. 3886–3892, 2006.

[4] F. Aghili, "A Robotic Testbed for Zero-G Emulation of Spacecraft," in *Proc. of 2005 IEEE Int. Conf. on Intelligent Robotics and Systems*, pp. 1033–1040, 2005.

[5] S. Dubowsky, W. Durfee, T. Corrigan, A. Kuklinski and U. Müller, "A Laboratory Test Bed for Space Robotics: The VES II," in *Proc. of 1994 IEEE Int. Conf. on Intelligent Robotics and Systems*, pp. 1562–1569, 1994.

[6] M. Inoue, J. Nakagawa and N. Arima, "Development of the Docking Dynamics Simulator," *Tran. Society of Instrument and Control Engineers*, Vol. 28, No. 11, pp. 1306–1313, 1992 (in Japanese).

[7] H. Shimoji, M. Inoue, N. Inaba and Y. Wakabayashi, "Evaluation of Space Robot Behavior Using Berthing Dynamics Simulator," *J. Robotics Society of Japan*, Vol. 13, No. 1, pp. 127–133, 1995 (in Japanese).

[8] A. Ejiri, I. Watanabe, K. Okabayashi, M. Hashima, M. Tatewaki, T. Aoki and T. Maruyama, "Satellite Berthing Experiment with a Two-Armed Space Robot," in *Proc. of 1994 IEEE Int. Conf. on Robotics and Automation*, pp. 3480–3487, 1994.

[9] Y. Nishimaki, D. Sato and M. Uchiyama, "Development of a Space Robot Teleoperation System Using a Hybrid Motion Simulator," in *Proc. of 2005 JSME Conf. on Robotics and Mechatronics*, 1A1-L1-17, 2004 (in Japanese).

[10] M. Uchiyama, K. Iimura, F. Pierrot, P. Dauchez, K. Unno and O. Toyama, "A New Design of a Very Fast 6-DOF Parallel Robot," in *Proc. of the 23rd Int. Symp. on Industrial Robots*, pp. 771–776, 1992.

[11] D. E. Rosenthal, "An Order n Formulation for Robotic Systems," *J. Astronautical Sciences*, Vol. 38, No. 4, pp. 511–529, 1990.